

## Multiple UAVs/UGVs heterogeneous coordinated technique based on Receding Horizon Control (RHC) and velocity vector control

DUAN HaiBin<sup>1,2\*</sup>, ZHANG YunPeng<sup>1,2</sup> & LIU SenQi<sup>2</sup>

<sup>1</sup>State Key Laboratory of Virtual Reality Technology and Systems, Beihang University, Beijing 100191, China

<sup>2</sup>Science and Technology on Aircraft Control Laboratory, School of Automation Science and Electrical Engineering, Beihang University, Beijing 100191, China

Received March 18, 2010; accepted November 30, 2010; published online February 28, 2011

Multiple unmanned air vehicles (UAVs)/unmanned ground vehicles (UGVs) heterogeneous cooperation provides a new breakthrough for the effective application of UAV and UGV. On the basis of introduction of UAV/UGV mathematical model, the characteristics of heterogeneous flocking is analyzed in detail. Two key issues are considered in multi-UGV subgroups, which are Reynolds Rule and Virtual Leader (VL). Receding Horizon Control (RHC) with Particle Swarm Optimization (PSO) is proposed for multiple UGVs flocking, and velocity vector control approach is adopted for multiple UAVs flocking. Then, multiple UAVs and UGVs heterogeneous tracking can be achieved by these two approaches. The feasibility and effectiveness of our proposed method are verified by comparative experiments with artificial potential field method.

**unmanned air vehicle (UAV), unmanned ground vehicle (UGV), Receding Horizon Control (RHC), Particle Swarm Optimization (PSO), velocity vector control**

Citation: Duan H B, Zhang Y P, Liu S Q. Multiple UAVs/UGVs heterogeneous coordinated technique based on Receding Horizon Control (RHC) and velocity vector control. *Sci China Tech Sci*, 2011, 54: 869–876, doi: 10.1007/s11431-010-4243-6

### 1 Introduction

Unmanned air vehicle (UAV) has the advantages of zero casualties, high-speed overload, good stealth performance, short operational preparation time, relatively low life-cycle cost. These advantages increase the capability of high-risk targets penetration, suppressing enemy air defense, deep target attacking and dominating the battle space. Unmanned ground vehicle (UGV) is generally capable of operating outdoors and over a wide variety of terrain, functioning in place of humans. Multiple UAVs can be used to cover large areas searching for targets. However, sensors on UAVs are typically limited in operating airspeed and altitude, combined with attitude uncertainty, placing a lower limit on their ability to resolve and localize ground features. UGVs

on the other hand can be deployed to accurately locate ground targets, but they have the disadvantage of not being able to move rapidly or see through such obstacles as buildings or fences. Therefore, multiple UAVs/UGVs heterogeneous cooperation provides a new breakthrough for the effective application of UAV and UGV [1–6]. Multiple UAVs and UGVs heterogeneous cooperation scenario can be shown with Figure 1.

For multiple UAVs/UGVs heterogeneous system, dynamic tracking is a typical problem. The ground moving target should be positioned dynamically and automatically, which make the target within the perception of the airborne camera [7]. Ref. [8] summarizes the two advanced research projects of about UAV rotorcraft and UGV cooperating in the battle space currently approved for funding by Defence R&D Canada. Ref. [9] proposed a cooperative control framework for a hierarchical UAV/UGV platform for wild-fire detection and fighting.

\*Corresponding author (email: hbduan@buaa.edu.cn)



**Figure 1** Multiple UAVs and UGVs heterogeneous cooperation scenario.

In order to realize the multiple UAVs and UGVs heterogeneous coordinated movement, the following control objectives should be satisfied:

- (1) The UGV subgroups should be in flocking motion.
- (2) The control center receives information from the UGV subgroups, and sends the central position information to the UAV subgroups at the same time.
- (3) The subgroups of multiple UAVs should follow and hover over the subgroups of multiple UGVs stably.

The constraints of the heterogeneous movements are as follows:

- (1) The subgroups of multiple UGVs could satisfy the Reynolds rule [10]: cohesion, separation, and alignment. In this way, the flocking movement can be realized.
- (2) The subgroups of multiple UAVs could receive the changing position center information of the UGV subgroups, and follow the movements of multiple UGVs.
- (3) The subgroups of multiple UAVs should avoid collisions during flight.

In this work, we present a Receding Horizon Control (RHC) approach for multiple UGVs, and velocity vector control approach for multiple UAVs. Multiple UAVs and UGVs heterogeneous tracking can be achieved by these approaches. The feasibility and effectiveness of our proposed method are verified by comparative experiments with artificial potential field method.

## 2 UAV/UGV mathematical model

In multiple UAV/UGV heterogeneous coordinated motion, UAVs and UGVs are all considered as particles. UGVs are moving on a plane, and the status variable of UGV<sub>*i*</sub> is  $x_{UGV_i}=(x_i, y_i, \dot{x}_i, \dot{y}_i)^T$ ,  $i=1,2,\dots, \text{NumUGV}$ . The motion equation can be expressed according to the following dynamics:

$$\begin{cases} \dot{r}_i = v_i, \\ \dot{v}_i = u_i. \end{cases} \quad (1)$$

For  $i=1,\dots, \text{NumUGV}$ ,  $r_i=(x_i, y_i)$  is the position vector of the *i*th UGV,  $v_i=(\dot{x}_i, \dot{y}_i)$  is the velocity vector, and  $u_{g_i}=(u_{x_i}, u_{y_i})$  is the control input. Thus the state vector of the *i*th UGV can be defined as  $x_{UGV_i}=(x_i, y_i, \dot{x}_i, \dot{y}_i)^T$ .

In the multiple UAVs flocking motion without a leader, all the UGVs have the same status, thus the velocity of the whole group is random when a stable and coordinated motion is achieved [11–15]. In this paper, a virtual UGV acting as a virtual leader (VL) is adopted to lead the whole UGV group to move in the right direction. The VL is a simulation of the instructions sent by the control center, and then received by each UGV. Since the VL will not be broken down, the instructions of the control center can be ensured to be executed by the UGV group. The motion equations of the VL are the same as those of the other UGVs, as shown in eq. (1), and its state vector is  $x_{vl}=(x_{vl}, y_{vl}, \dot{x}_{vl}, \dot{y}_{vl})^T$ , where  $r_{vl}=(x_{vl}, y_{vl})$  and  $v_{vl}=(\dot{x}_{vl}, \dot{y}_{vl})$ .

In the heterogeneous coordinated motion, the UAV group will follow the UGV group. The state vector of the *j*th UAV is:  $x_{UGV_j}=(v_j, \gamma_j, \chi_j, x_j, y_j, z_j)^T$  for  $j=1,\dots, \text{NumUAV}$ , and its control inputs are thrust  $T_j$ , load factor  $n_j$  and bank angle  $\mu_j$ . The following equations are adopted as the dynamic model of UAV:

$$\begin{cases} \dot{v} = g[(T - D) / W - \sin \gamma], \\ \dot{\gamma} = (g / v)(n \cos \mu - \cos \gamma), \\ \dot{\chi} = (gn \sin \mu) / (v \cos \gamma), \\ \dot{x} = v \cos \gamma \cos \chi, \\ \dot{y} = v \cos \gamma \sin \chi, \\ \dot{z} = -v \sin \gamma, \end{cases} \quad (2)$$

where  $v$  is the airspeed of UAV,  $\gamma$  is the flight path angle,  $\chi$  the flight path heading,  $x$ ,  $y$ , and  $z$  denote the position,  $g$  denotes the acceleration of gravity,  $D$  denotes the drag, and  $W$  denotes the weight.

## 3 Multiple UGVs coordinated control based on RHC

The initial speed and direction of each UGV in the group are different from each other, the designed controller should make the UGVs gradually meet Reynolds rule in the motion of following the VL, the effect of multi-UGV cooperative movement must be achieved. For the *i*th UGV, the control input is:  $u_{g_i}=(u_{x_i}, u_{y_i})$ ,  $i=1,2,\dots, \text{NumUGV}$ . The control input of the whole UGV group can be defined as  $U_{UGV}=(u_{g_1}, u_{g_2}, \dots, u_{g_{\text{NumUGV}}})=\{U_{UGV}(t) \mid \forall t \in [0, T]\}$ , and the state of the whole UGV group is  $X_{UGV}=(x_{UGV_1}, x_{UGV_2}, \dots,$

$X_{UGV, NumUGV}) \in \mathfrak{R}^{4 \times NumUGV}$ . Thus the multi-UGV motion equations can be described as

$$\dot{X}_{UGV}(t) = f(t, X_{UGV}(t), U_{UGV}(t)). \quad (3)$$

Let  $X_{UGV}(0) = X_{0UGV}$  represent the initial state of the UGV group, then the state at any time  $t \in (0, T]$  can be determined by the following equation:

$$X_{UGV}(t) = X_{UGV}(0) + \int_0^t f(\tau, X_{UGV}(\tau), U_{UGV}(\tau)) d\tau. \quad (4)$$

If the initial states are definite,  $X_{UGV}(t)$  can only be obtained by  $U_{UGV}$ , which can be also expressed by  $X_{UGV}(t | U_{UGV})$ .

In the research on flocking conducted by Tanner and Olfati-Saber [16, 17], the cohesion and separation rules of Reynolds are satisfied by designing a proper artificial potential field. Each UGV matches its velocity to its neighbors, and the alignment rule can be fully satisfied. For the flocking motion following a VL, the control input of each UGV ( $u_i, i=1, 2, \dots, NumUGV$ ) will include an additional part to coordinate its position and velocity with the VL.

There are complexities and diversities of control objectives in the movement of multiple UGVs heterogeneous movement, which orient the optimal control strategy from the unconstrained quadratic optimization problem to multi-objective optimization problem. RHC has been proved to be more successfully optimized online in a dynamic environment, which is based on the simple idea of repetitive solution of an optimal control problem and state updating after the first input of the optimal command sequence. The main idea of RHC is the online receding/moving optimization. It breaks the global control problem into several local optimization problems of smaller sizes, which can significantly decrease the computing complexity and computational expense. Particle Swarm Optimization (PSO) is a population based stochastic optimization technique, which is inspired by social behavior of bird flocking or fish schooling. It is demonstrated that PSO can find better results in a faster, cheaper way compared with other methods. Hybrid RHC and PSO approach is developed for multiple UGVs movement in this work.

Consider searching space with  $n$  dimensions, the particle population is  $m$ , and the position of the  $i$ th particle can be expressed with  $X_i = (X_{i1}, X_{i2}, \dots, X_{in})$ , and the velocity is  $V_i = (V_{i1}, V_{i2}, \dots, V_{in})$ . The current best solution is  $P_i = (P_{i1}, P_{i2}, \dots, P_{in})$ , and the global best solution is  $P_g = (P_{g1}, P_{g2}, \dots, P_{gn})$ . For the  $t$ th generation, the position and velocity updating rule can be expressed as follows:

$$\begin{aligned} V_i(t+1) &= \chi \cdot (V_i(t) + c_1 \cdot r_1 \cdot (P_i(t) - X_i(t)) + c_2 \cdot r_2 \cdot (P_g(t) - X_i(t))), \\ X_i(t+1) &= X_i(t) + V_i(t+1), \end{aligned} \quad (5)$$

where  $r_1$  and  $r_2$  are two independent random numbers between (0,1);  $c_1$  and  $c_2$  are two learning factors;  $\chi$  is a constant number between (0,1). The objective function for RHC

can be expressed as follows:

$$\begin{aligned} \min_u J &= f(X_{UGV}, U_{UGV}; t_c, T_p) \\ J &= \int_{t_c}^{t_c+T_p} F(X_{UGV}, U_{UGV}) dt \\ \text{subject to } \dot{X}_{UGV} &= f(t, X_{UGV}, U_{UGV}) \\ LL_{UGV} &\leq \begin{bmatrix} X_{UGV} \\ U_{UGV} \end{bmatrix} \leq UL_{UGV} \end{aligned} \quad (6)$$

where  $t_c$  is control horizon,  $T_p$  is predictive horizon, and  $t_c \leq T_p$ ;  $LL_{UGV}$  and  $UL_{UGV}$  denote the upper and lower bound respectively.

The topology of the wireless network connecting the UGVs is an adjacency graph  $G = \{V, E\}$  [16, 17]. The set of vertices  $V = \{n_1, n_2, \dots, n_{NumUGV}\}$  represent the UGVs and the set of edges  $E = \{(n_i, n_j) \in V \times V \mid n_i - n_j\}$  represent the adjacency relation between the UGVs. Let  $A = (a_{ij})$  denote the adjacency matrix of  $G$ , then  $a_{ij} \neq 0 \Leftrightarrow (i, j) \in E$ , and  $A$  is symmetric,  $A^T = A$ . Let  $N_i$  denote the set of the UGVs that are adjacent to the  $i$ th UGV:

$$N_i = \{j \in V : a_{ij} \neq 0\} = \{j \in V : (i, j) \in E\}. \quad (7)$$

Let  $R_{UGV}$  represent the maximum detecting range of a UGV, and  $R_{UGV} > 0$ , thus  $N_i$  can be described as

$$N_i = \{j \in V : \|r_i - r_j\| \leq R_{UGV}\}, \quad (8)$$

where  $\|\cdot\|$  is the Euclidean norm. Then, for  $R_{UGV} > 0$ , the set of edges  $E$  can be described as

$$E = \{(i, j) \in V \times V : \|r_i - r_j\| < R_{UGV}, i \neq j\}. \quad (9)$$

(1) Potential cost. A potential field is established between UGVs in order that the cohesion and separation rules can be satisfied. The potential function between UGV $_i$  and UGV $_j$  is  $V_{ij}$  (see Figure 2).  $V_{ij}$  is a nonnegative, differentiable and unbounded function of the distance  $\|r_i - r_j\|$ .  $V_{ij}$  obtains its unique minimum when the distance  $\|r_i - r_j\|$  is the desired distance  $d_{UGV}$ .

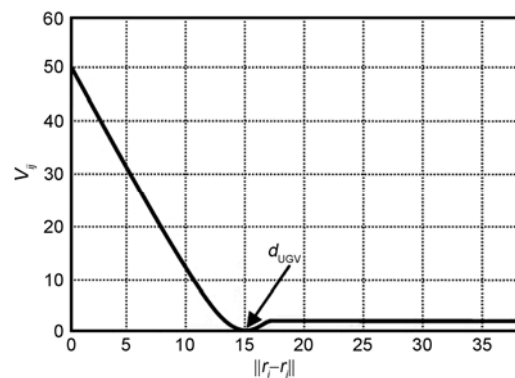


Figure 2 The curve of the potential function  $V_{ij}$ .

$$V_{ij} = \frac{1}{2} \sum_i \sum_{j \neq i} \psi(\|r_i - r_j\|). \tag{10}$$

In this work, we adopt the potential function introduced by Reza, and define the  $\sigma$ -norm [16] as follows:

$$\|x\|_\sigma = \frac{1}{\xi} \left[ \sqrt{1 + \xi \|x\|^2} - 1 \right], \tag{11}$$

where, the constant  $\xi > 0$ . The gradient of  $\sigma$ -norm can be expressed by

$$\sigma_\xi(x) = \frac{x}{\sqrt{1 + \xi \|x\|^2}} = \frac{x}{1 + \xi \|x\|_\sigma}. \tag{12}$$

According to the definition of  $\sigma$ -norm,  $V_{ij}$  can also be re-written as  $V\sigma_{ij}$ :

$$V\sigma_{ij} = \frac{1}{2} \sum_i \sum_{j \neq i} \psi_\alpha(\|r_i - r_j\|_\sigma). \tag{13}$$

When  $\|r_i - r_j\| \geq R_{UGV}$ , the following function of  $\varphi_\alpha(\|r_i - r_j\|)$  is introduced [17]:

$$\begin{aligned} \varphi_\alpha(\|r_i - r_j\|) &= \rho_h(\|r_i - r_j\| / \|R_{UGV}\|_\sigma) \varphi(\|r_i - r_j\| - \|d_{UGV}\|), \\ \varphi(x) &= \frac{1}{2} [(a+b)\sigma_1(x+c) + (a-b)], \end{aligned} \tag{14}$$

where  $\sigma_1(x) = x / \sqrt{1+x^2}$ ;  $a, b, c$  satisfy  $b \gg a > 0, c = |a-b| / \sqrt{4ab}$ , and  $\varphi(0)=0$ .

$$\rho_h(x) = \begin{cases} 1 & x \in [0, h), \\ \frac{1}{2} \left[ 1 + \cos \left( \pi \frac{(x-h)}{(1-h)} \right) \right] & x \in [h, 1], \\ 0 & \text{otherwise,} \end{cases} \tag{15}$$

where  $h \in (0, 1)$ .

$\psi_\alpha(\|r_i - r_j\|)$  and  $\varphi_\alpha(\|r_i - r_j\|)$  satisfy the following equation:

$$\psi_\alpha(\|r_i - r_j\|) = \int_{\|d_{UGV}\|}^{\|r_i - r_j\|} \varphi_\alpha(s) ds. \tag{16}$$

Then, the collective potential cost of the whole UGV group can be described as

$$F_{\text{potential}} = \sum_{i=1}^{\text{NumUGV}} \sum_{j \in N_i} \varphi_\alpha(\|r_i - r_j\|_\sigma) n_{ij}, \tag{17}$$

where  $n_{ij} = \sigma_\xi(r_j - r_i)$ .

The UGVs will maneuver to lower the collective potential, until the group converges to a stable and coordinated flocking motion, which has the lowest collective potential.

(2) Consensus cost. Each UGV will match its velocity

with its neighboring flockmate to satisfy the alignment rule. The consensus cost is defined as

$$F_{\text{consensus}} = \sum_{i=1}^{\text{NumUGV}} \sum_{j \in N_i} |a_{ij}(r)(v_j - v_i)|, \tag{18}$$

where  $a_{ij}(r)$  in the adjacent matrix  $A$  can be obtained by

$$a_{ij}(r) = \rho_h(\|r_j - r_i\|_\sigma / \|R_{UGV}\|_\sigma) \in [0, 1], \quad j \neq i. \tag{19}$$

When the multiple UGVs match their velocities with neighbors, the consensus cost of the whole group will be lowered. When a stable flocking motion is achieved, the consensus cost  $F_{\text{consensus}}$  is close to zero.

(3) Following cost. All the UGVs should regulate their motions to follow the VL, thus the following cost is defined as

$$F_{\text{follow}} = \sum_{i=1}^{\text{NumUGV}} |c_1(r_i - r_v)| + |c_2(v_i - v_v)|, \quad c_1, c_2 > 0. \tag{20}$$

In the multiple UGVs flocking motion, each UGV follows a VL, and the UGVs will regulate their velocity according to the position and velocity of the VL to lower the following cost.

Finally, the cost function of RHC can be described as

$$F(X_{UGV}, U_{UGV}) = F_{\text{potential}} + F_{\text{consensus}} + F_{\text{follow}}. \tag{21}$$

This cost function will be used as the total objective function, which can be optimized by PSO algorithm. The solution is the optimal control input of each UGV, which will lower the cost value of the whole group gradually, and lead to a coordinated flocking motion.

#### 4 Multiple UGVs coordinated control based on velocity vector control

According to the heterogeneous mission requirements, the multiple UAV subgroups need stability in the movement to follow and hover over the multiple UGVs, and each UAV should avoid collision during flight. In this way, the multiple UAVs and UGVs heterogeneous coordinated movement is formed.

According to the control input  $ua_i = (T_i, n_i, \mu_i)$ , where  $i=1, 2, \dots, \text{NumUAV}$ ,  $T_i$  denotes the thrust of UAV $_i$ ,  $n_i$  denotes the overload, and  $\mu_i$  denotes the banking angle. The input control vector can be expressed with  $U_{\text{UAV}} = (ua_1, ua_2, \dots, ua_{\text{NumUAV}}) = \{U_{\text{UAV}}(t) \mid \forall t \in [0, T]\}$ , and the state vector can be defined as  $X_{\text{UAV}} = (x_{\text{UAV}1}, x_{\text{UAV}2}, \dots, x_{\text{UAVNumUAV}}) \in \mathfrak{R}^{6 \times \text{NumUAV}}$ . Then, the dynamics for UAV can be written as follows:

$$\dot{X}_{UGV}(t) = f(t, X_{UGV}(t), U_{UGV}(t)). \tag{22}$$

The control policy of changing the control input of  $U_{\text{UAV}}$

into velocity vector  $U_{UAV}$  can ensure that all agents eventually align with each other and have a common heading direction while at the same time avoid collisions and group into a tight formation [18], and  $\bar{v}_c = (\bar{v}_{c1}, \bar{v}_{c2}, \dots, \bar{v}_{c \text{NumUAV}})$ . The velocity vector  $\bar{v}_{ci}$  of UAV<sub>*i*</sub> includes velocity  $v_{ci}$ , banking angle  $\gamma_{ci}$ , and yaw angle  $\chi_{ci}$ , i.e.  $\bar{v}_{ci} = (v_{ci}, \gamma_{ci}, \chi_{ci})$ . Suppose the velocity vector satisfies the following equations:

$$\begin{aligned} \dot{v}_{ci} &= \omega_v(v_{ci} - v_i), \\ \dot{\gamma}_{ci} &= \omega_\gamma(\gamma_{ci} - \gamma_i), \\ \dot{\chi}_{ci} &= \omega_\chi(\chi_{ci} - \chi_i), \end{aligned} \tag{23}$$

where  $\omega_v$ ,  $\omega_\gamma$  and  $\omega_\chi$  are gain constants corresponding to velocity, banking angle and yaw angle respectively.

According to eqs. (2) and (23), the thrust  $T_{ci}$  can be obtained as follows:

$$T_{ci} = D_i + \omega_v W_i (v_{ci} - v_i) / g + W_i \sin \gamma_i. \tag{24}$$

The overload  $n_{ci}$  can be expressed with

$$n_{ci} = \sqrt{(\omega_\gamma v_i (\gamma_{ci} - \gamma_i) + \cos \gamma_i)^2 + (\omega_\chi v_i (\chi_{ci} - \chi_i) \cos \gamma_i / g)^2}. \tag{25}$$

The pitch angle  $\mu_{ci}$  can be expressed with

$$\mu_{ci} = \arctan \left( \frac{\omega_\chi v_i (\chi_{ci} - \chi_i) \cos \gamma_i / g}{\omega_\gamma v_i (\gamma_{ci} - \gamma_i) + \cos \gamma_i} \right). \tag{26}$$

The resistance  $D_i$  can be obtained according to the following equation:

$$D_i = 0.5 v_i^2 S C_{D0} + 2 k n^2 W_i^2 / (\rho v_i^2 S), \tag{27}$$

where  $S$  denotes the reference square of UAV,  $C_{D0}$  denotes zero lift drag coefficient,  $k$  denotes the induced drag coefficient,  $\rho$  denotes the density of atmosphere.

The corresponding velocity vector can be expressed as following:

$$\bar{v}_{ci} = c_a \bar{v}_{ai} + c_{ic} \bar{v}_{tci}, \tag{28}$$

where  $\bar{v}_{ai}$  and  $\bar{v}_{tci}$  denote collision avoidance vector and hovering velocity vector respectively,  $i=1, 2, \dots, \text{NumUAV}$ ,  $c_a$  and  $c_{ic}$  are the corresponding weight coefficients, and  $0 < c_a < 1, 0 < c_{ic} < 1, c_a + c_{ic} = 1$ .

(1) Collision avoidance velocity vector. Multiple UAVs hover over multiple UGVs, and collision should be avoided to ensure safe flight of UAV. The collision avoidance strategy of priority mechanism is adopted in this section. The priority number level is assigned to each UAV in the multi-UAV groups, and the small number with high priority, the UAV<sub>*i*</sub> with low priority can avoid the UAV<sub>*j*</sub> ( $j < i$ ) with high priority. The collision avoidance velocity vector  $\bar{v}_{ai}$  of the UAV<sub>*i*</sub> with low priority can be calculated by the average velocity of UAV<sub>*i*</sub> and UAV<sub>*j*</sub>, and the direction of

$\bar{v}_{ai}$  is pointing to UAV<sub>*i*</sub> along the UAV<sub>*j*</sub> (see Figure 3).

The weight coefficient  $c_a$  of collision avoidance is decided by the distance  $da_{ij}$  between two UAVs and the security collision distance  $d_{avoid}$ , which can be expressed by

$$c_a = \exp(|da_{ij} - d_{avoid}| / \sigma_a), \tag{29}$$

where  $\sigma_a > 0$ , and  $0 < c_a < 1$ .

(2) Track hovering velocity vector. Multiple UAVs subgroup can receive messages from the control center, and position the center of UGV subgroups. Suppose the minimum hovering velocity of UAV is  $v_{min}$ , the hovering velocity is  $\omega_{circle}$ , and the minimum hovering radius can be expressed by  $r_{circle} = v_{min} / \omega_{circle}$ . The track hovering velocity vector depends on the distance  $d_{tc}$  between UAV<sub>*i*</sub> and the center  $C$  in the horizontal direction.

**Case 1.** When  $d_{tc} > 3r_{circle}$ , UAV<sub>*i*</sub> is far away from multi-UGV subgroups, the vector  $\bar{v}_{tci}$  may maintain the current velocity value or increase a little. The direction points to the center  $C$  of multi-UGV subgroups (see Figure 4, marked with ★).

**Case 2.** When  $d_{tc} \leq 3r_{circle}$ , UAV<sub>*i*</sub> hovers in the vicinity of multi-UGVs with  $\bar{v}_{tci}$ . When the direction and speed of UAV<sub>*i*</sub> are the same with the multiple UGV subgroups, we can determine whether UAV<sub>*i*</sub> follows the center  $C$ . If yes,

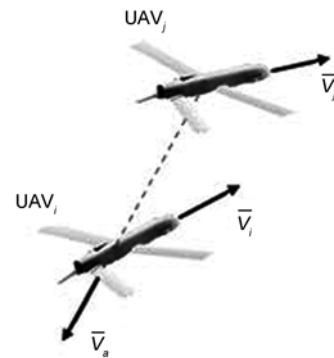


Figure 3 The collision avoidance velocity vector  $\bar{v}_{ai}$  of UAV<sub>*i*</sub>.

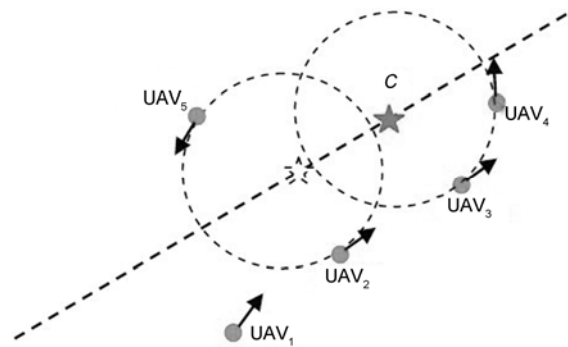


Figure 4 Multiple UAV subgroups hovering over the center  $C$  of multiple UGV subgroups.

then UAV<sub>i</sub> continues to hover in the vicinity of multi-UGVs. Otherwise, UAV<sub>i</sub> will follow the center C. In the following process, UAV<sub>i</sub> maintains the same value or increases a little, while the direction keeps unanimous with the multiple UGVs (see Figure. 4). With  $\vec{v}_{ai}$  and  $\vec{v}_{ci}$ , the velocity vector  $\vec{v}_{ci}$  of UAV<sub>i</sub> can be obtained by eq. (28), and the vector command group  $\vec{v}_c$  of multiple UAV subgroup can also be obtained.

Multiple UAVs and UGVs heterogeneous cooperation process can be illustrated by Figure 5.

**5 Experimental results**

The feasibility and effectiveness of our proposed method

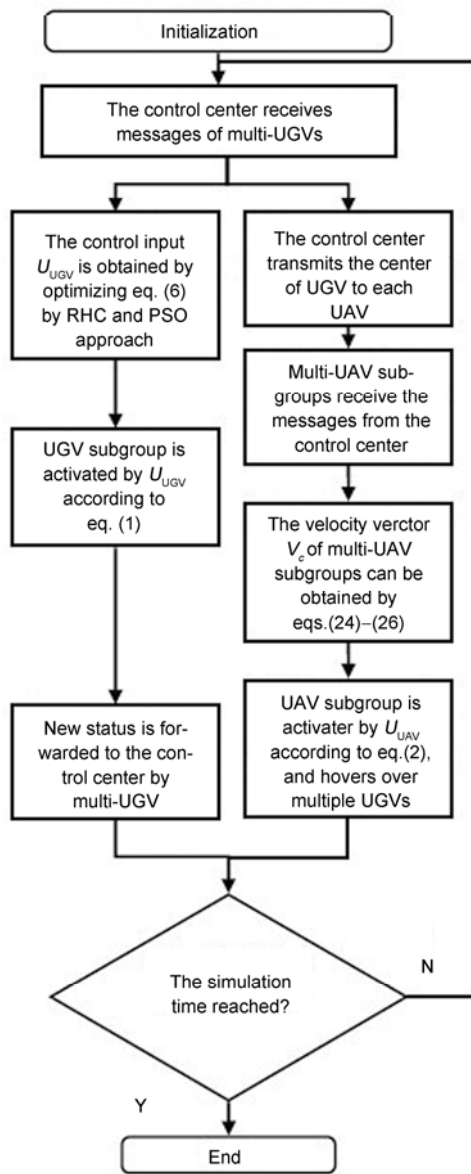


**Figure 5** Flowchart of multiple UAVs and UGVs heterogeneous cooperation.

are verified by series of comparative experiments with artificial potential field method. In the experiments, there are 6 UAVs, 10 UGVs and 1 control center. The initialized parameters of multiple UGV subgroup are set as follows:  $d_{UGV}=15, R_{UGV}=1.2d_{UGV}, \zeta=0, a=5, b=5, h=0.9, c_1=1, c_2=1, T_p=3s, \delta=1s, t_c=1s. ps=20, w_{max}=1.2, w_{min}=0.1, vp_{max}=4, pc_1=0.5, pc_2=0.5, Nc_{max}=80.$

The initialized parameters of multiple UAV subgroup are set as follows:  $\rho=1.25 \text{ kg/m}^3, W=14400 \text{ kg},$  the reference square= $30 \text{ m}^2, T_{max}=15000 \text{ kg}, n_{max}=7, k=0.1, C_{D0}=0.02, \omega_v=1, \omega_\gamma=0.2, \omega_\chi=1, g=9.8 \text{ m/s}^2. v_{min}=100 \text{ m/s}, v_{max}=200 \text{ m/s}, \omega_{circle}=(\pi/12) \text{ rad/s}, \omega_{\chi_{max}}=(\pi/9) \text{ rad/s}, \omega_{\gamma_{max}}=(\pi/9) \text{ rad/s}. d_{avoid}=30\text{m}, \sigma_a=10.$

The initialized position of VL in multiple UGV subgroup is (1020, 1020) m, the initialized velocity is 25 m/s. The initialized status of multiple UGV subgroup and VL are shown with Figure 6 (“■” denotes VL).

The initialized status of multiple UAV subgroup is listed in Table 1, and the initialized status of multiple UAV subgroup is shown with Figure 7 (“●” denotes UAV).

Figure 8 gives the multiple UAVs and UGVs heterogeneous cooperation results by using artificial potential field method.

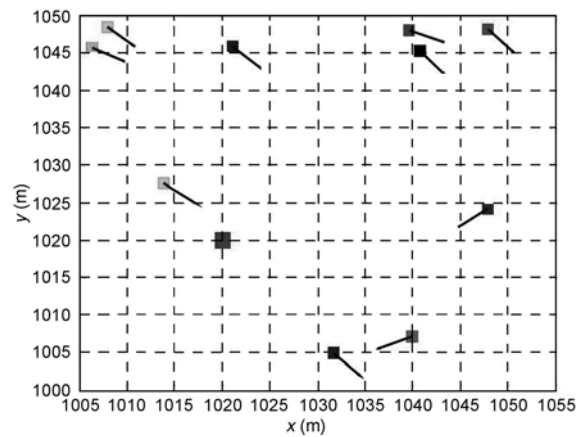


**Figure 6** The initialized status of multiple UGV subgroup and VL.

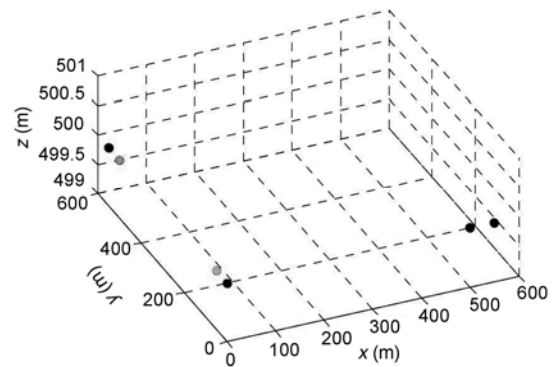


**Figure 7** The initialized status of multiple UAV subgroup.

**Table 1** The initialized status of multiple UAV subgroup

UAV No.	$V$ (m/s)	$\gamma$ (rad)	$\chi$ (rad)	$x, y, z$ (m)
1	120	$\pi/18$	0	550, 0, 500
2	120	$\pi/18$	0	500, 0, 500
3	120	0	0	0, 500, 500
4	120	0	0	0, 0, 500
5	120	0	0	0, 550, 500
6	120	0	0	0, 50, 500

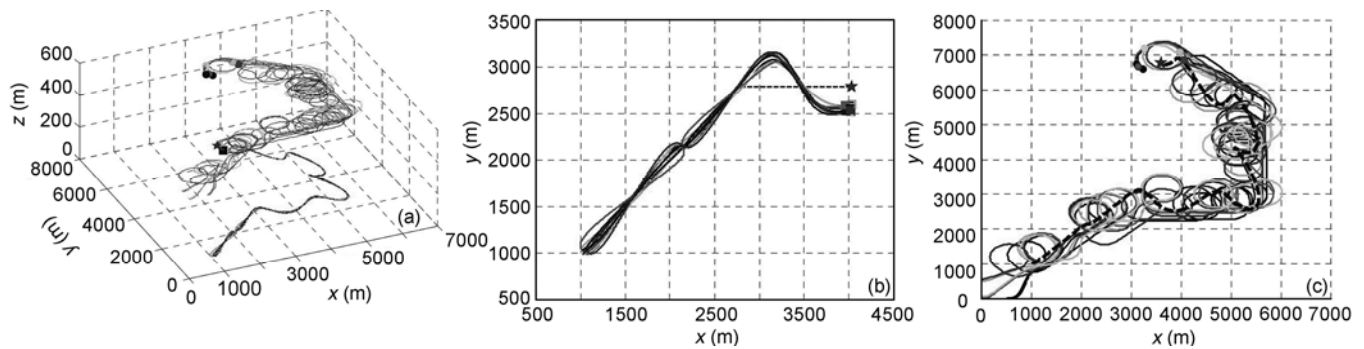
Figure 8 gives the multiple UAVs and UGVs heterogeneous cooperation results by using artificial potential field method.

Figure 9 gives the multiple UAVs and UGVs heterogeneous cooperation results by the hybrid method proposed in this paper.

The results in Figures 8 and 9 demonstrate that the proposed approach in this paper can guarantee stable convergence, robust tracking, and high efficiency. It clearly shows the superiority of the proposed algorithm over the traditional artificial potential field method. Simulations with different conditions are also conducted to verify the feasibility and effectiveness of the proposed controller.

## 6 Conclusions

Multiple UAVs/UGVs heterogeneous cooperation provides a new breakthrough for the effective application of UAV and UGV [19, 20]. This paper proposed a RHC approach for multiple UGVs, and a velocity vector control approach for multiple UAVs, and multiple UAVs and UGVs heterogeneous tracking can be achieved by these two approaches. The superiority of our proposed method is also verified by comparative experiments with artificial potential field method. Our future work will focus on applying the new approach proposed in this paper to real-world multiple UAVs/UGVs heterogeneous cooperation. In a real-time application, it is difficult to neglect solution times for the optimization algorithm that must be run at every step. However, with faster computers and improved technology, the proposed approach can be a good candidate for real-time formation control of multiple UAVs/UGVs heterogeneous cooperation under various complicated environments. Furthermore, bio-inspired intelligence [21] also provides a novel way for multiple UAVs/UGVs heterogeneous cooperation.



**Figure 8** Multiple UAVs and UGVs heterogeneous cooperation results by using artificial potential field method. (a) Traces of multiple UAVs and UGVs heterogeneous cooperation; (b) traces of multiple UGV subgroup before 150 s; (c) traces of multiple UAV subgroup before 150 s.

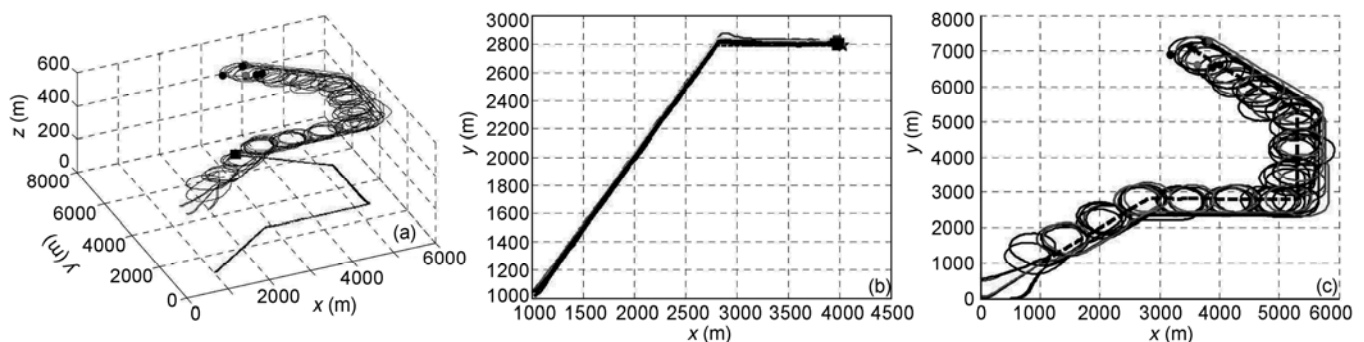


**Figure 9** Multiple UAVs and UGVs heterogeneous cooperation results by the hybrid method proposed in this paper. (a) Traces of multiple UAVs and UGVs heterogeneous cooperation; (b) traces of multiple UGV subgroup following VL before 150 s; (c) Traces of multiple UAV subgroup before 150 s.

This work was supported by the National Natural Science Foundation of China (Grant Nos. 60975072 and 60604009), Aeronautical Science Foundation of China (Grant No. 2008ZC01006), Program for New Century Excellent Talents in University of China (Grant No. NCET-10-0021), the Fundamental Research Funds for the Central Universities of China (Grant No. YWF-10-01-A18), Beijing NOVA Program Foundation (Grant No. 2007A017), open Fund of the State Key Laboratory of Virtual Reality Technology and Systems, and Open Fund of the Provincial Key Laboratory for Information Processing Technology, Suzhou University, China (Grant No. KJS1020).

- 1 Tanner H G, Christodoulakis D. Cooperation between aerial and ground vehicle groups for reconnaissance missions. Proceeding of the 45th IEEE Conference on Decision and Control, San Diego: IEEE, 2006. 5918–5923
- 2 Grocholsky B, Bayraktar S, Kumar V, et al. Synergies in feature localization by air-ground robot teams. Proceeding of the 2004 International Symposium on Experimental Robotics. Singapore: Springer, 2004. 353–362
- 3 Chaimowicz L, Cowley A, Gomez-Ibanez D, et al. Deploying air-ground multi-robot teams in urban environments. Proceedings of the 3rd International Workshop on Multi-Robot Systems, Washington D C: Springer, 2005, 3: 223–234
- 4 Loyall J, Schantz R, Corman D, et al. A distributed real-time embedded application for surveillance, detection, and tracking of time critical targets. Proceeding of the 2005 IEEE Real Time and Embedded Technology and Applications Symposium, San Francisco: IEEE, 2005. 88–97
- 5 Hsieh M A, Chaimowicz L, Cowley A, et al. Adaptive teams of autonomous aerial and ground robots for situational awareness. *J Field Robotics*, 2007, 24(11-12): 991–1014
- 6 Rudol P, Wzorek M, Conte G, et al. Micro unmanned aerial vehicle visual serving for cooperative indoor exploration. Proceeding of the 2008 IEEE Aerospace Conference. Montana: IEEE, 2008. 1–10
- 7 Ariyur K B, Fregene K O. Autonomous tracking of a ground vehicle by a UAV. Proceedings of American Control Conference, Seattle, Washington: IEEE, 2008. 669–671
- 8 Michael T, Blake B. Semi-autonomous UAV/UGV for dismounted urban operations. Proceedings of SPIE, vol 7692. Orlando: SPIE, 2010. 76921C
- 9 Phan C, Liu H T. A cooperative UAV/UGV platform for wildfire detection and fighting. Proceedings of 2008 Asia Simulation Conference - 7th International Conference on System Simulation and Scientific Computing. Beijing: IEEE, 2008. 494–498
- 10 Reynolds C. Flocks, birds, and schools: a distributed behavior model. *Computer Graphics*, 1987, 21(4): 25–34
- 11 Vicsek T, Czirok A, Jacob E B, et al. Novel type of phase transitions in a system of self-driven particles. *Phys Rev Lett*, 1995, 75(6): 1226–1229.
- 12 Jadbabaie A, Lin J, Morse A S. Coordination of groups of mobile autonomous agents using nearest neighbor rules. *IEEE Trans Automatic Control*, 2002, 48(6): 988–1001
- 13 Tanner H G, Jadbabaie A, Pappas G J. Coordination of multiple autonomous agents. Proceeding of the 11th IEEE Mediterranean Conference on Control and Automation. Greece: IEEE, 2003. 3448–3453
- 14 Palejjiya D, Tanner H G. Hybrid velocity/force control for robot navigation in compliant unknown environments. *Robotica*, 2006, 24(6): 745–758
- 15 Tanner H G. Flocking with obstacle avoidance in switching networks of interconnected vehicles. Proceeding of 2004 IEEE International Conference on Robotics and Automation. Barcelona: IEEE, 2004. 3006–3011.
- 16 Tanner H G, Jadbabaie A, Pappas G J. Stable flocking of mobile agents. part I: fixed topology. Proceeding of the 42nd IEEE Conference on Decision and Control. Hawaii: IEEE, 2003. 2010–2015
- 17 Saber O R. Flocking for multi-agent dynamic systems: algorithms and theory. *IEEE Trans Automatic Control*, 2006, 51(3): 401–420
- 18 Gowtham G, Kumar K S. Simulation of multi UAV flight formation. Proceeding of the 24th IEEE/AIAA Digital Avionics Systems Conference. Washington DC: IEEE, 2005. 11. A.3-1–11.A.3-6
- 19 Duan H B, Liu S Q. Unmanned air/ground vehicles heterogeneous cooperative techniques: current status and prospects. *Sci China Tech Sci*, 2010, 53(5): 1349–1355
- 20 Duan H B, Ding Q X, Liu S Q, et al. Time-delay compensation of heterogeneous network control for multiple UAVs and UGVs. *J Internet Technol*, 2010, 11(3): 379–385
- 21 Duan H B, Zhang X Y, Xu C F. Bio-inspired Computing (in Chinese). Beijing: Science Press, 2011